



Cheng Xu,¹ Yu Cai,¹ Pengcheng Fan,¹ Bo Bai,¹ Jie Chen,¹ Han-Bing Deng,¹ Chi-Ming Che,² Aimin Xu,¹ Paul M. Vanhoutte,¹ and Yu Wang¹



Calorie Restriction Prevents Metabolic Aging Caused by Abnormal SIRT1 Function in Adipose Tissues

Diabetes 2015;64:1576–1590 | DOI: 10.2337/db14-1180

Adipose tissue is a pivotal organ determining longevity, due largely to its role in maintaining whole-body energy homeostasis and insulin sensitivity. SIRT1 is a NAD-dependent protein deacetylase possessing antiaging activities in a wide range of organisms. The current study demonstrates that mice with adipose tissue-selective overexpression of hSIRT1(H363Y), a dominant-negative mutant that disrupts endogenous SIRT1 activity, show accelerated development of metabolic aging. These mice, referred to as Adipo-H363Y, exhibit hyperglycemia, dyslipidemia, ectopic lipid deposition, insulin resistance, and glucose intolerance at a much younger age than their wild-type littermates. The metabolic defects of Adipo-H363Y are associated with abnormal epigenetic modifications and chromatin remodeling in their adipose tissues, as a result of excess accumulation of biotin, which inhibits endogenous SIRT1 activity, leading to increased inflammation, cellularity, and collagen deposition. The enzyme acetyl-CoA carboxylase 2 plays an important role in biotin accumulation within adipose tissues of Adipo-H363Y. Calorie restriction prevents biotin accumulation, abolishes abnormal histone biotinylation, and completely restores the metabolic and adipose functions of Adipo-H363Y. The effects are mimicked by short-term restriction of biotin intake, an approach potentially translatable to humans for maintaining the epigenetic and chromatin remodeling capacity of adipose tissues and preventing aging-associated metabolic disorders.

Advancing age is associated with loss of energy balance and deterioration of metabolic functions. In older people, postprandial hyperglycemia is common (1). The prevalence of glucose intolerance and insulin resistance increases

progressively and significantly with age (2). The redistribution of fat from subcutaneous depots to visceral compartment and from adipose tissues to ectopic sites plays a critical role in the development of aging-related metabolic abnormalities, in particular type 2 diabetes. Older people exhibit elevated central fat deposition but decreased skeletal muscle mass (referred to as sarcopenic obesity) (3). Preadipocytes isolated from aged animals and humans have a reduced potential to differentiate and replicate, whereas aged adipocytes show a decreased capacity for lipid storage (4). The mechanisms underlying age-associated changes in adipose tissue function and fat distribution remain incompletely understood.

SIRT1 is a mammalian ortholog most closely related to SIR2 (silent information regulator 2), a protein identified in *Saccharomyces cerevisiae* that extends replicative life span (5). Both SIRT1 and SIR2 belong to a conserved family of aging regulators and are NAD-dependent deacetylases that catalyze the removal of acetyl groups from protein substrates (6). In yeast, SIR2 acts as a transcriptional silencer by modulating histone modifications, especially at the mating-type loci and telomeric DNA regions (7). These chromosome domains are analogous to the heterochromatin of multicellular eukaryotes. When a conserved histidine within the catalytic domain of SIR2 was converted to a tyrosine (H364Y), its histone modification activity was lost and the mutant acted in a strong dominant-negative manner (8). Compared with SIR2, SIRT1 elicits a wider range of biological functions by interacting with and regulating diversified protein substrates (5).

Animal studies reveal that SIRT1 is a key energy sensor controlling cellular responses to nutrient availability and in

¹State Key Laboratory of Pharmaceutical Biotechnology and Department of Pharmacology and Pharmacy, The University of Hong Kong, Hong Kong, China

²Department of Chemistry and Chemical Biology Center, Jockey Club Building for Interdisciplinary Research, The University of Hong Kong, Hong Kong, China

Corresponding author: Yu Wang, yuwanghk@hku.hk.

Received 1 August 2014 and accepted 27 November 2014.

This article contains Supplementary Data online at <http://diabetes.diabetesjournals.org/lookup/suppl/doi:10.2337/db14-1180/-/DC1>.

© 2015 by the American Diabetes Association. Readers may use this article as long as the work is properly cited, the use is educational and not for profit, and the work is not altered.

turn protecting against aging-related metabolic diseases (9). SIRT1 is critically involved in the metabolic adaptation to fasting, exercise, and calorie restriction (10), which upregulate the activity of this antiaging protein in adipocytes and adipose tissues (11). Activation of SIRT1 in turn stimulates fat mobilization and adiponectin production in adipose tissues (12–14). Overexpression of SIRT1 in adipose tissues of mice induces a phenotype similar to that with calorie restriction (leaner and metabolically more active, with improved insulin sensitivity and glucose tolerance [14–16]). This evidence suggests that adipose SIRT1 is a candidate drug target for promoting systemic energy homeostasis and healthy aging.

Transgenic mice that selectively overexpress wild-type (WT) human SIRT1 (hSIRT1) or hSIRT1(H363Y) mutant in adipose tissues have been established (14). In the current study, the metabolic functions of these two types of transgenic mice, referred to as Adipo-SIRT1 and Adipo-H363Y, respectively, are compared and related to those of the WT controls. Whereas Adipo-SIRT1 are more insulin sensitive and metabolically healthier than their WT littermates (14), Adipo-H363Y exhibit a phenotype of accelerated metabolic aging. Calorie restriction has been applied to test whether or not this nongenetic intervention is able to restore a normal metabolic function in Adipo-H363Y. The results demonstrate that a large number of aging-induced changes of gene expression in adipose tissues are prevented by calorie restriction, which significantly delays the development of insulin resistance, glucose intolerance, and dyslipidemia in both WT and Adipo-H363Y. Limited biotin intake contributes to the beneficial effects of calorie restriction on enhancing SIRT1 activity in adipose tissues and improving systemic energy homeostasis. At the epigenetic level, by preventing excessive histone biotinylation, calorie restriction facilitates SIRT1-mediated histone deacetylation and transcriptional silencing.

RESEARCH DESIGN AND METHODS

Animal Experiments

All procedures were approved by the Committee on the Use of Live Animals for Teaching and Research of The University of Hong Kong and carried out in accordance with ARRIVE (Animal Research: Reporting of In Vivo Experiments) as well as institutional guidelines for the care and use of laboratory animals. The generation of transgenic mice with selective overexpression of human SIRT1 (Adipo-SIRT1) or hSIRT1(H363Y) (Adipo-H363Y) in adipose tissues was previously described (14). Mice were housed in a room under controlled temperature ($23 \pm 1^\circ\text{C}$) and 12-h light-dark cycles, with free access to water and standard mouse chow (4.07 kcal/g composed of 20% protein, 52.9% carbohydrate, 5.6% fat, 4.7% fiber, 6.1% minerals, and vitamin mixture containing 0.3 mg/kg biotin; LabDiet 5053; LabDiet, Purina Mills, Richmond, IN). All animals appeared normal and were fertile, giving rise to healthy litters. Male mice were used for the current study.

The food intake for ad libitum-fed mice was ~ 0.14 g/g body weight/day. For calorie restriction, mice received 60% of the normal food supply (~ 0.08 g/g body weight/day) from the age of 10–40 weeks. To study the effects of biotin intake in the diet, mice were given either biotin-sufficient (4.11 kcal/g composed of 18% casein, 60% sucrose, 10% vegetable oil, 2% corn oil, 4% salt, and vitamin mixture containing 0.45 mg/kg biotin; 02960407; MP Biomedicals, Santa Ana, CA) or biotin-deficient (4.11 kcal/g composed of 18% casein, 60% sucrose, 10% vegetable oil, 2% corn oil, 4% salt, and vitamin mixture without biotin; 02901030; MP Biomedicals) diets. Mice were randomly assigned to each experimental group ($n = 8$ –10) for diet treatment starting at the age of 10 weeks. Metabolic parameters were monitored on a weekly basis.

For *in vivo* RNA interference (RNAi) treatment, three sets of chemically modified silencing RNAs (siRNAs) for acetyl-CoA carboxylase (ACC)2 were synthesized by RiboBio (Guangdong, China), including sense 5'-CCUACGA GAUGUCCGUAAdTdT-3'/antisense 3'-dTdTGGGAUGCUC UACAAGGCAUU-5', sense 5'-GCAUCAAGUAUGCUCUCA AdTdT-3'/antisense 3'-dTdTTCGUAGUUCACGAGAGUU-5', and sense 5'-CCACCUAUGUGUACGACUAdTdT-3'/antisense 3'-dTdTGGUGGAUACACAUGCUGAA-5'. Mice were treated with the mixture of ACC2 siRNAs (5 nmol/mouse/day) or the same amount of scrambled RNAi by intraperitoneal injection at six different sites for three consecutive days (17). The epididymal adipose tissues were harvested 12 h after the last injection for subsequent analysis.

Metabolic Evaluations

Body weight, blood glucose, and fat mass composition were measured between 1000 and 1200 h for mice that were either starved overnight or fed ad libitum. Blood glucose was monitored by tail nicking using an Accu-Check Advantage II Glucometer (Roche Diagnostics, Mannheim, Germany). The body composition was assessed in conscious and unanesthetized mice using a Bruker minispec Body Composition Analyzer (Bruker Optics, Inc., Woodlands, TX). The intraperitoneal glucose tolerance test (ipGTT) and insulin tolerance test (ITT) were performed as previously described (14,18). Circulating and tissue contents of lipids, including triglycerides, total cholesterol, and free fatty acids, were analyzed using LiquiColor Triglycerides and Stanbio Cholesterol (Stanbio Laboratory, Boerne, TX) and the Half-Micro Test Kit (Roche Diagnostics), respectively. The fasting serum insulin concentration was quantified using the commercial ELISA kits from Mercodia AB (Uppsala, Sweden). Serum adiponectin and lipocalin-2 concentrations were determined with the in-house ELISA kit as previously described (19,20). Metabolic rate (VO_2 , VCO_2 , and respiratory exchange ratio [RER]) was measured by indirect calorimetry using a six-chamber open-circuit Oxymax system component of the Comprehensive Laboratory Animal Monitoring System (CLAMS; Columbus Instruments, Columbus, OH) as previously described

(14). All mice were acclimatized to the cage for 48 h before recording the parameters during a 2-day feeding and a 24-h fasting period.

Microarray Analysis

Total RNA was extracted from epididymal adipose tissues of WT, Adipo-SIRT1, and Adipo-H363Y mice aged 8 and 40 weeks using the RNeasy Mini Kit (Qiagen, Valencia, CA). Samples were derived from at least three mice in each group. The quality of RNA was assessed by a spectrophotometer (ND-1000, Nanodrop Technologies, Wilmington, DE) and the RNA 6000 Pico LabChip with the Agilent 2100 Bioanalyzer (Agilent Technologies, Palo Alto, CA). The A260-to-A280 ratios of all RNA samples were between 1.9 and 2.1. The RNA integrity numbers were >9. After reverse transcription, the labeled cDNA samples were hybridized to the Mouse Genome 430 2.0 expression arrays using the GeneChip Fluidics Station 450 (Affymetrix Inc., Santa Clara, CA). The intensity of the probed signals was scanned and captured by GeneChip Scanner 3000 (Affymetrix Inc.). Quality of the raw intensity data was assessed using diagnostic plots by GeneSpring GX 12.6 (Agilent Technologies) and Affymetrix Expression Console (Affymetrix Inc.). Raw intensity values of gene expression were normalized and background corrected using the Robust Multiarray Average algorithm. Genes with expression values lower than the 20th percentile of all intensity values were excluded from further analyses. The expression profiles of samples derived from WT, Adipo-SIRT1, and Adipo-H363Y were clustered and validated by principal component analysis. Data comparisons were performed between 1) 8-week-old WT, Adipo-SIRT1, and Adipo-H363Y; 2) 40-week-old WT, Adipo-SIRT1, and Adipo-H363Y fed ad libitum; 3) 8- and 40-week-old ad libitum-fed mice of the same genotypes; and 4) 8- and 40-week-old mice of the same genotypes under calorie restriction. Differentially expressed genes were defined as more than a twofold change using a generalized linear model. In total, a list of 3,915 genes that were changed in at least one set of the above comparisons is included in Supplementary Table 1 for further analysis. Venn diagrams were used for presenting the numbers of differentially or commonly changed genes. The MIAME-compliant microarray data have been submitted to and are available in the ArrayExpress database (www.ebi.ac.uk/arrayexpress, accession number E-MTAB-2777).

Quantitative Reverse Transcription PCR

Quantitation of target genes was performed using SYBR Green PCR Master Mix (Qiagen) and an ABI PRISM 7900 HT Sequence Detection System (Applied Biosystems, Foster City, CA). The primer sequences are listed in Supplementary Table 2. Data were calculated and are presented as relative expression of transcripts normalized to β -actin.

Chromatin Immunoprecipitation-PCR

The primers for chromatin immunoprecipitation-PCR (ChIP-PCR) are listed in Supplementary Table 2. The histone acetylation and/or biotinylation at the promoter regions of different genes were analyzed and compared

by ChIP-PCR as previously described with modifications (21). In brief, epididymal adipose tissue (100 mg) was minced into small pieces in cold PBS (137 mmol/L NaCl, 4.3 mmol/L Na_2HPO_4 , 2.7 mmol/L KCl, 1.4 mmol/L KH_2PO_4 , pH 7.4) with protease inhibitor cocktails. Formaldehyde was added to a final concentration of 1%, and the mixture was incubated at room temperature for 15 min with moderate shaking. The cross-linking was stopped by adding glycine to a final concentration of 0.125 mol/L. The nuclei were isolated from the tissue lysates and resuspended in lysis buffer (1% SDS, 50 mmol/L Tris-HCl, pH 8.0, 10 mmol/L EDTA, containing protease inhibitors) for sonication to obtain chromatin fragments of 500–1,000 bp. After preclearing with protein G-Sepharose beads (Pierce, Rockford, IL) (blocked with 0.2 mg/mL salmon sperm DNA and 0.5 mg/mL BSA), 50 μg chromatin was incubated with 2 μg antibody overnight at 4°C. Immune complexes were collected on protein G-Sepharose beads (blocked as above), washed, and eluted into 100 μL ChIP elution buffer (1% SDS and 0.1 mol/L NaHCO_3). Half of the elutes were reverse cross-linked and the other half diluted 1:10 with lysis buffer to perform the second ChIP with streptavidin-conjugated beads (Pierce) as previously described (22). After elution with ChIP elution buffer, the cross-link was reversed by adding 8 μL of 5 mol/L NaCl and incubating for 4 h at 65°C. The DNA was purified by phenol-chloroform extraction. PCR amplifications were performed using 10% of the DNA samples and the resulting PCR products separated by agarose gel for image quantification by densitometry (MultiAnalyst Software; Bio-Rad). Quantitation was also performed by quantitative reverse transcription PCR analysis. The results were normalized against those from either the input DNA samples or the first ChIP fractions and presented as fold changes.

SIRT1 Activity Measurements

SIRT1 activity was monitored using a Fluorometric Drug Discovery kit (Enzo Life Sciences International, Inc., Plymouth Meeting, PA). Fluorescence was measured with a fluorometric reader (CytofluorII 400 series; Applied Biosystems), whereby excitation was set at 360 nm and emission detection at 460 nm. The *in vitro* protein deacetylation assay was analyzed by high-performance liquid chromatography as previously described (14). The histone H3 peptides, including ARTKQTARKSTGG K¹⁴APRK¹⁸QLC with or without acetylation at K¹⁴ and/or biotinylation at K¹⁸, were used as substrates. In brief, recombinant SIRT1 (3.6 $\mu\text{mol/L}$) was incubated with peptide substrate (500 $\mu\text{mol/L}$) and NAD⁺ (500 $\mu\text{mol/L}$) in 50 mmol/L Tris buffer (pH 7.5) at 37°C for 10 min, in the presence and absence of 500 $\mu\text{mol/L}$ biotin. Trifluoroacetic acid was added to 0.1% before fractionation by reverse-phased high-performance liquid chromatography on a Symmetry C18 column (5 μm , 3.9 \times 150 mm; Waters, Milford, MA), using a 40-min linear gradient (0–40% buffer B containing acetonitrile with 0.5% trifluoroacetic acid) at a flow rate of 1

mL/min. Chromatographic peaks were detected by an ultraviolet detector at 214 nm. The sizes of the peaks obtained by calculating the areas under the peaks were used for comparison.

Quantification of Tissue Biotin Contents

The amount of total biotin (bound and unbound) was determined as previously described (23) with modifications. In brief, 30 mg of tissue or cell lysates was hydrolyzed in sulfuric acid at 100°C for 1 h. After neutralization, 3.5 mg of activated charcoal was added to bind the liberated biotin. The mixture was centrifuged at 12,000 rpm for 3 min, and the bound biotin was released by adding 1 mL of 5% ammonia ethanol solution. The supernatant was filtered and evaporated to dryness under nitrogen. The extract was reconstituted in 100 μ L methanol and mixed with 80 μ L of 0.1% 9-anthryldiazomethane (ADAM, weight for volume in ethyl acetate) for 1 h at room temperature. The fluorescent biotin-ADAM was detected at an excitation wavelength of 365 nm and emission wavelength of 412 nm using the fluorometric reader. Biotin solutions (1–50 ng/mL) were used to generate a standard curve for calibration and quantification.

Histological Analysis

Paraffin sections (5 μ m) were prepared for adipose tissues collected from different groups of mice. Hematoxylin and eosin staining was performed to analyze adipocyte histology under a light microscope (Olympus, Tokyo, Japan). The sizes of adipocytes were measured as previously described (18). Masson trichrome staining was performed using Accustain Trichrome Kits (Sigma-Aldrich, St. Louis, MO) to evaluate the extracellular deposition of fibrillar collagens.

Western Blotting

Antibodies against total ACC, ACC2, histone H3, histone H4, acetylated histone H3 (K9), and acetylated lysine were purchased from Cell Signaling (Beverly, MA). Antibodies against ACC1, SIRT1, and acetylated histone H4 (K5, K8, K12, and K16) were from Millipore (Billerica, MA). Monoclonal antibodies against β -actin and streptavidin-horseradish peroxidase (HRP) conjugate were obtained from Sigma-Aldrich. For Western blotting, proteins derived from cell or tissue lysates were separated by SDS-PAGE and transferred to polyvinylidene difluoride membranes. After overnight blocking, membranes were probed with various primary antibodies followed by secondary antibodies. Immunoreactive antibody-antigen complexes were visualized with the enhanced chemiluminescence reagents from GE Healthcare (Uppsala, Sweden). For histone modification analysis, histones were extracted from the nuclear fractions of epididymal fat pads following a previously reported procedure (21). In brief, the pellets of nuclei were resuspended overnight in 0.4 mol/L H₂SO₄ at 4°C. The supernatant was collected after centrifugation (16,000g, 10 min at 4°C) and precipitated with trichloroacetic acid at 4°C for 1 h. The acid-soluble histone fraction was subjected to 18% SDS-PAGE and visualized by Coomassie Brilliant Blue staining. The biotinylated protein was detected by Western blotting using streptavidin-HRP conjugate,

and the acetylated protein detected with antiacetyl-lysine antibodies.

Data Analysis

The density of protein bands in Western blots was analyzed quantitatively using ImageJ 1.45 software (National Institutes of Health, Bethesda, MD) for calculating the expression ratios against loading controls. Representative Western blotting images are shown. Statistical calculations were performed with the Statistical Package for the Social Sciences version 11.5 software package (SPSS, Inc., Chicago, IL). For multiple comparisons, the differences were analyzed by one-way ANOVA, followed by Dunnett test. Differences in other comparisons were determined by an unpaired two-tailed Student *t* test. In all cases, statistically significant differences were accepted when *P* values were <0.05. All results were derived from at least three sets of independent experiments unless otherwise specified. Data are presented as mean \pm SEM.

RESULTS

Overexpression of hSIRT1(H363Y) in Adipose Tissue Accelerates the Development of Metabolic Aging

The metabolic parameters, including body weight, blood glucose, serum insulin, and circulating lipid levels, were monitored on a weekly basis. Systemic insulin sensitivity was evaluated by ITTs and ipGTTs. Compared with both WT and Adipo-SIRT1, Adipo-H363Y showed a phenotype of significantly accelerated metabolic aging (Fig. 1). At as early as the age of 20 weeks, abnormal responses to ITT and ipGTT were detected in Adipo-H363Y when compared with age-matched WT (Supplementary Fig. 1). At the age of 30 weeks, the responses of Adipo-H363Y to either ITT or ipGTT were comparable to those of 60-week-old WT (Fig. 1A). By contrast, these responses in 60-week-old Adipo-SIRT1 were not significantly different from mice at the age of 30 weeks. Although the body weight was not significantly different between the three groups of mice at the age of 12 weeks, Adipo-H363Y showed a consistently higher gain of body weights than the other two groups of mice at other age points (Fig. 1B). Fasting glucose levels of Adipo-H363Y were not significantly different from WT (data not shown). However, from the age of 40 weeks onwards, the nonfasting glucose levels were significantly higher in Adipo-H363Y than in the other two groups of mice (Fig. 1C). Circulating insulin levels were rapidly rising with age, being higher in Adipo-H363Y by \sim 51, \sim 79, and \sim 85% than those of WT at the age of 20, 40, and 60 weeks, respectively (Fig. 1D). The insulin concentration in 30-week-old Adipo-H363Y reached a level similar to that in WT at 60 weeks of age. Circulating triglyceride levels augmented progressively in both Adipo-H363Y and WT but remained the lowest in Adipo-SIRT1 (Fig. 1E). Compared with WT, the development of aging-associated hypertriglyceridemia was enhanced significantly by \sim 19, \sim 21, and \sim 31% in Adipo-H363Y at 40, 50, and 60 weeks of age, respectively.

In line with their higher body weight gain, Adipo-H363Y showed significantly increased (by >10%) whole-body

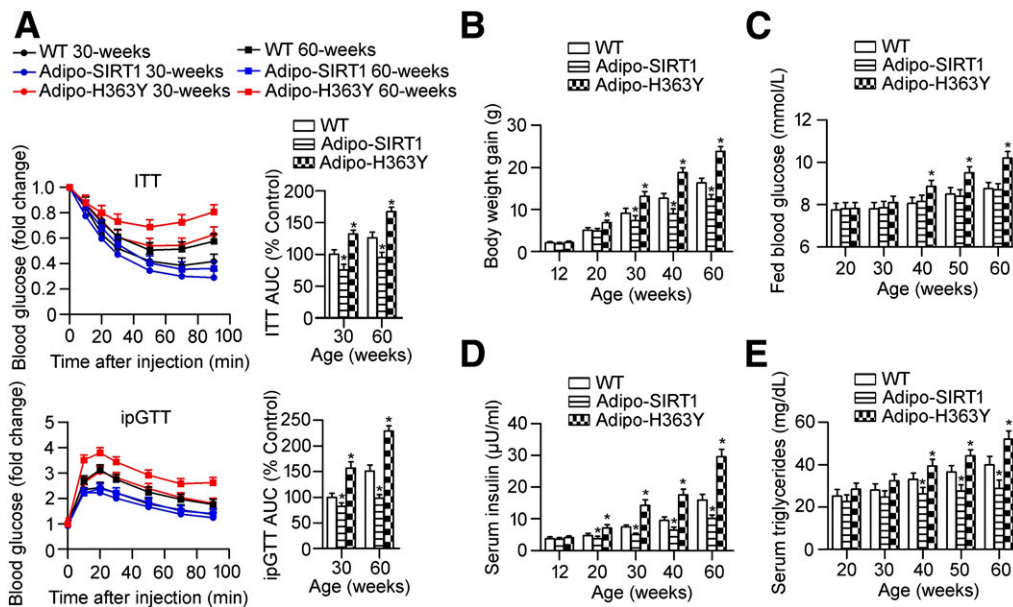


Figure 1—Overexpression of hSIRT1(H363Y) in adipose tissue accelerates the development of metabolic aging in mice. *A*: ITTs and ipGTTs were performed and compared between 30- and 60-week-old WT, Adipo-SIRT1, and Adipo-H363Y. *B*: Body weight was recorded after overnight fasting and the body weight gain calculated by referring to those of WT, Adipo-SIRT1, and Adipo-H363Y at the age of 8 weeks. *C*: Blood glucose was recorded at 1000 h in mice fed ad libitum. *D*: Circulating insulin levels were measured in sera collected from WT, Adipo-SIRT1, and Adipo-H363Y after overnight fasting. *E*: Mice were killed at different ages, and the fasting serum triglyceride concentration was measured. * $P < 0.05$, compared with the corresponding WT group ($n = 8$).

adiposity from the age of 20 weeks onwards when compared with WT, whereas changes in opposite directions were observed in Adipo-SIRT1 (decreased by ~20%) (Fig. 2A). However, the percentage compositions of lean and fluid mass were not significantly different between WT and Adipo-H363Y (Supplementary Fig. 2). On the other hand, the weights of visceral fat pads collected postmortem were not elevated in Adipo-H363Y when compared with those in WT (Fig. 2B), indicating that the excess lipids were deposited in ectopic sites. Indeed, the triglyceride contents in liver and skeletal muscle of Adipo-H363Y were augmented significantly by ~35 and ~61%, respectively, when compared with WT (Fig. 2C). In adipose tissues of Adipo-H363Y, the cholesterol and free fatty acid contents were significantly higher (by 1.5- and 1.9-fold, respectively) than in those of WT (Fig. 2C). However, the size of adipocytes in epididymal adipose tissues of Adipo-H363Y was significantly smaller (Supplementary Fig. 3). Histological assessment showed an increased cellularity and trichrome-positive streaks interspersed between adipocytes in adipose tissues of Adipo-H363Y (Supplementary Fig. 4A). The expressions of genes involved in adipogenesis were significantly downregulated, whereas those associated with inflammation were upregulated in adipose tissues of Adipo-H363Y (Supplementary Fig. 4B). Indirect calorimetric analysis revealed that the RER was elevated significantly in Adipo-H363Y during both dark and light periods (Fig. 2D). The increased RER in Adipo-H363Y was attributed mainly to the higher CO_2 production (VCO_2) but not to differences in O_2 consumption (VO_2).

Collectively, the results demonstrate that overexpression of hSIRT1(H363Y) selectively in adipose tissues of mice accelerates the development of insulin resistance, glucose intolerance, postprandial hyperglycemia, and dyslipidemia, a cluster of metabolic defects that are closely associated with aging.

Calorie Restriction Restores the Metabolic Functions of WT and Adipo-H363Y

Total SIRT1 protein expression was decreasing with age in adipose tissues of WT but remained higher in those of Adipo-SIRT1 and Adipo-H363Y (Fig. 3A). Compared with that of WT, SIRT1 activity was significantly augmented (by approximately twofold) in adipose tissues of Adipo-SIRT1 but decreased (by ~60%) in those of Adipo-H363Y (Fig. 3B). Compared with mice at the age of 12 weeks, SIRT1 activities were decreased by ~35, ~10, and ~55% in 40-week-old WT, Adipo-SIRT1, and Adipo-H363Y, respectively. Calorie restriction (60% of ad libitum food intake) for 30 weeks not only prevented the downregulation of SIRT1 activities but also significantly enhanced the latter in adipose tissues of both WT and Adipo-H363Y (Fig. 3C). At the age of 40 weeks, mice under calorie restriction showed similar levels of SIRT1 activity in their adipose tissues, which was elevated by ~2.1- and ~4.3-fold compared with the corresponding ad libitum-fed WT and Adipo-H363Y, respectively. Calorie restriction significantly reduced the nonfasting glucose levels in all mice (Fig. 3D) and improved the responses to ITT and ipGTT in both WT and Adipo-H363Y (Fig. 3E). The area under the

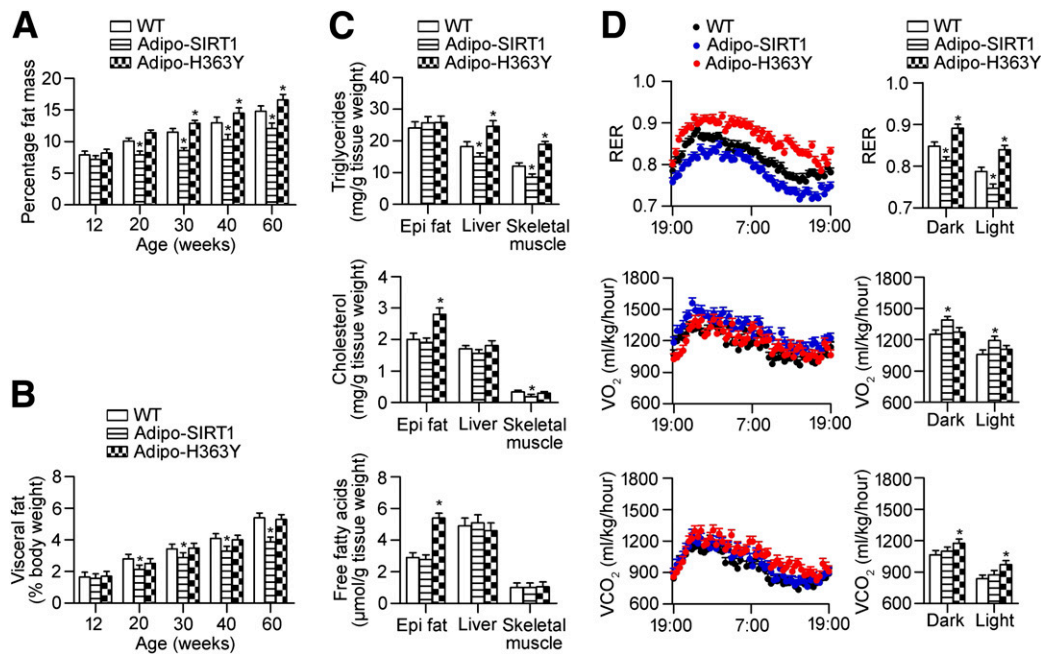


Figure 2—Selective overexpression of hSIRT1(H363Y) in adipose tissues leads to augmented body fat mass and ectopic lipid accumulation. *A*: Body fat composition (fat content/body weight %) was analyzed and compared in WT, Adipo-SIRT1, and Adipo-H363Y from different age-groups. The results are calculated as percentage values of the body weights. *B*: The wet weights of epididymal and perirenal fat pads were recorded and combined to calculate the percentage amounts of visceral fat compared with the total body weight. *C*: Triglycerides (upper), cholesterol (middle), and free fatty acids (bottom) were measured in epididymal (epi) fat, liver, and skeletal muscle collected from WT, Adipo-SIRT1, and Adipo-H363Y (40 weeks old, fasted for 16 h). *D*: Indirect calorimetry analysis was performed to obtain the RER, VO₂, and VCO₂ values in WT, Adipo-SIRT1, and Adipo-H363Y (30 weeks old, fed ad libitum) (light period 0700–1900 h). **P* < 0.05, compared with corresponding WT (*n* = 10).

curve (AUC) values of ipGTT and ITT in calorie-restricted WT and Adipo-H363Y were not significantly different from those of age-matched Adipo-SIRT1 (Fig. 3E, bottom panels). At the age of 40 weeks, the body weight gain and plasma insulin levels in the three groups of mice under calorie restriction were not significantly different (Fig. 3F), and were comparable to those in 20-week-old WT (Fig. 1B and D).

Calorie-restricted WT, Adipo-SIRT1, and Adipo-H363Y exhibited similar diurnal rhythmic patterns of RER, ~0.82 in dark cycles and ~0.75 in light cycles (Fig. 4A). The VCO₂ of Adipo-H363Y was significantly decreased by calorie restriction in both dark (~14%) and light (~23%) cycles, to levels comparable to those in WT and Adipo-SIRT1 (Fig. 4A). The whole-body adiposity was similar in the three types of mice across all age-groups under calorie restriction (Fig. 4B). The percentage weights of postmortem visceral fat pads in calorie-restricted mice at the age of 40 weeks were comparable to those in 20-week-old mice fed ad libitum (Fig. 4B and Fig. 2B). The aging-induced augmentation of circulating triglyceride levels was prevented by calorie restriction in WT and Adipo-H363Y (Fig. 4C). Calorie restriction significantly reduced the lipid contents in adipose tissues of all mice groups (Fig. 4D) and attenuated the ectopic lipid deposition in Adipo-H363Y (Fig. 4E).

Together, these findings suggest that despite the decreased SIRT1 activity in adipose tissues of Adipo-H363Y, calorie restriction can correct both local and

systemic metabolic defects caused by adipose overexpression of the mutant hSIRT1(H363Y) and/or aging.

Increased Histone Biotinylation Causes Abnormal Chromatin Remodeling in Adipose Tissues of Adipo-H363Y

Microarray analysis was performed using RNA samples extracted from adipose tissues of mice at the age of either 8 weeks (referred to as “young,” when metabolic functions were comparable among the three groups) or 40 weeks (referred to as “old,” when significant differences in metabolic functions were obvious). Principal component analysis of the adipose transcriptome revealed that samples derived from young WT, Adipo-SIRT1, and Adipo-H363Y could be separated into three distinct clusters (Supplementary Fig. 5A). The number of differentially expressed (by more than twofold) transcripts was obtained by pairwise comparison between mice of the same age-group or between young and old mice of the same genotype (3,915 genes in total) (Supplementary Table 1). Compared with young WT, 1,390 and 429 genes were differentially expressed in adipose tissues of age-matched Adipo-SIRT1 and Adipo-H363Y, respectively (Supplementary Fig. 5B). Over 90% (1,269) of the altered gene expressions in young Adipo-SIRT1 were due to upregulation (Supplementary Fig. 6A). In adipose tissues of Adipo-H363Y, genes related to cholesterol biosynthesis were significantly upregulated and those of mitochondrial fatty acid oxidation

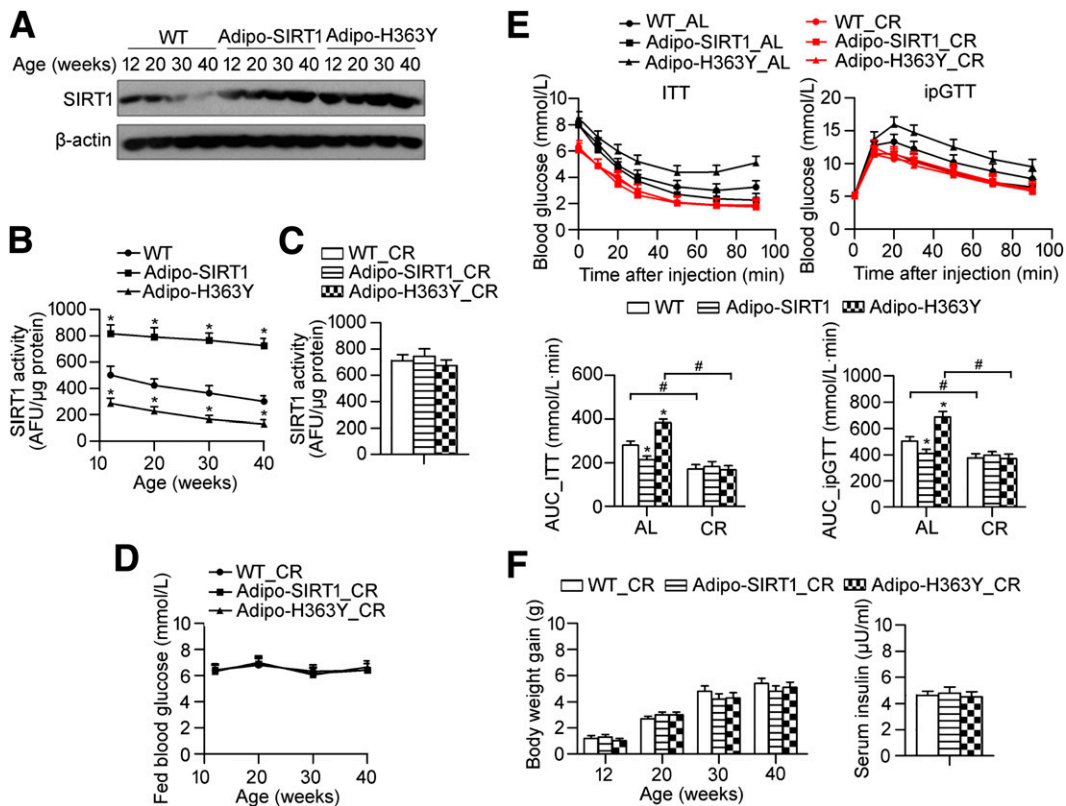


Figure 3—Caloric restriction prevents aging- and/or hSIRT1(H363Y) overexpression-induced metabolic defects in WT and Adipo-H363Y. **A:** Protein expression of SIRT1 was monitored in epididymal fat lysates of WT, Adipo-SIRT1, and Adipo-H363Y by Western blotting using an antibody recognizing both the murine and human species of this protein. **B:** A Fluorometric Drug Discovery Kit was used to measure the SIRT1 activity in epididymal fat pads collected from different age-groups of WT, Adipo-SIRT1, and Adipo-H363Y. For each sample, tissue lysates containing 20 μ g of proteins were used. Fluorescent readings are presented as arbitrary fluorescence unit (AFU) in equal amount of proteins for comparison. **C:** SIRT1 activity was determined in epididymal fat pads collected from WT, Adipo-SIRT1, and Adipo-H363Y subjected to 30 weeks of calorie restriction (CR). **D:** Blood glucose was recorded at 1000 h for mice under calorie restriction and compared across different groups. **E:** ITT (top left) and ipGTT (top right) were performed in \sim 30-week-old WT, Adipo-SIRT1, and Adipo-H363Y either fed ad libitum (AL) or subjected to calorie restriction. The AUCs are compared (bottom left and right, respectively). **F:** Body weight gain was calculated as in Fig. 1B for WT, Adipo-SIRT1, and Adipo-H363Y subjected to calorie restriction from the age of 12 weeks onwards (left). Fasting (16 h) insulin concentration (right) was measured using sera samples collected from 40-week-old WT, Adipo-SIRT1, and Adipo-H363Y under calorie restriction. * $P < 0.05$, compared with the corresponding WT group; # $P < 0.05$, compared with the corresponding ad libitum group ($n = 8$).

significantly downregulated (Supplementary Fig. 6B). With the progression of aging, different patterns of changes in adipose gene expression were observed in the three types of mice (Fig. 5A). In general, the genome expression and chromatin state in adipose tissues of Adipo-H363Y were more rigid than the other two groups of mice. The average gene expression levels in adipose tissues of young WT, Adipo-SIRT1, and Adipo-H363Y were 0.210, 0.746, and 0.061, respectively. Compared with the corresponding young mice, a significant decrease was observed in the average gene expression level of old Adipo-SIRT1 (-0.081), whereas that of old Adipo-H363Y decreased slightly to 0.041 (Fig. 5A). Compared with those of WT (1,107) and Adipo-SIRT1 (2,425), less (901) numbers of genes were changed by aging (more than twofold) in adipose tissues of old Adipo-H363Y (Supplementary Fig. 7, top panels). In addition to those involved in sterol lipid metabolism, genes encoding extracellular matrix

and tight junction proteins were further upregulated in old Adipo-H363Y (Supplementary Fig. 7, bottom panel). A larger number (2,425) of genes were changed in old compared with young Adipo-SIRT1, with \sim 70% downregulated, suggesting a more flexible and dynamic chromatin structure in adipose tissues of these mice (Supplementary Figs. 7 and 8). Calorie restriction prevented \sim 45 and \sim 36% of aging-induced gene changes in adipose tissues of WT and Adipo-H363Y, respectively. Especially, out of the 103 genes upregulated in old Adipo-H363Y adipose tissues, 93 (\sim 90%) were prevented by calorie restriction (Supplementary Fig. 8, top left panel). Among those that remained unchanged (two-fold or less) during aging, 888 and 1,029 were altered by calorie restriction (more than twofold) in WT and Adipo-H363Y, respectively (Supplementary Fig. 7, top right panel). About 47 and 60% of genes changed by calorie restriction (more than twofold) in WT and Adipo-H363Y,

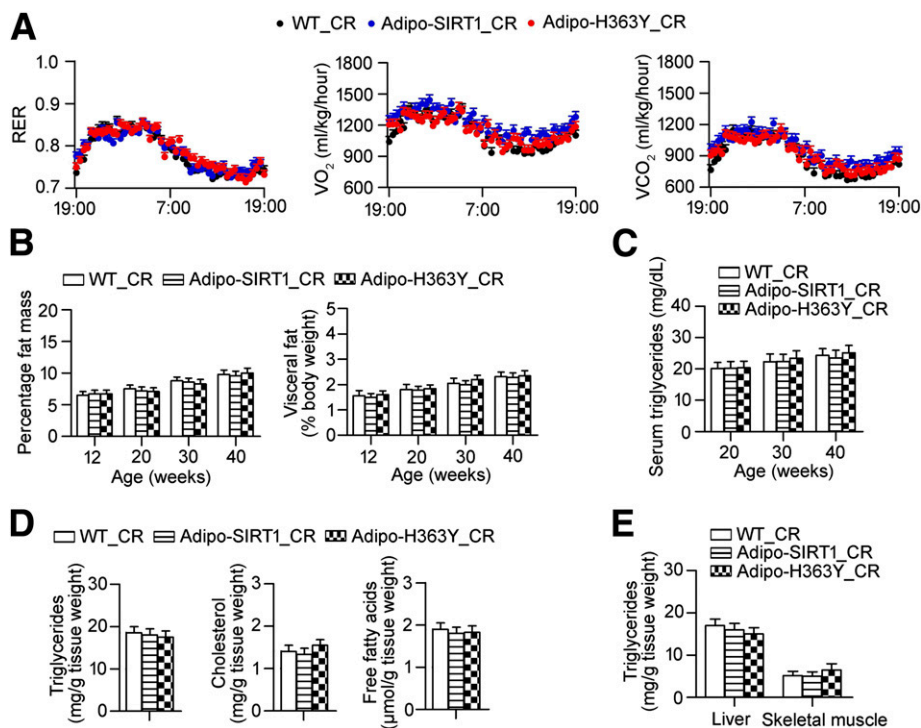


Figure 4—Caloric restriction restores the metabolic capacity and reduces ectopic lipid accumulation in Adipo-H363Y. **A:** Indirect calorimetric analysis was performed in 30-week-old WT, Adipo-SIRT1, and Adipo-H363Y under calorie restriction (light period 0700–1900 h). **B:** Percentage body fat mass (total fat content/body weight %, left panel) and visceral fat (epididymal and per renal fat/body weight %, right panel) were measured and calculated for calorie-restricted WT, Adipo-SIRT1, and Adipo-H363Y as in Fig. 2. **C:** Serum triglyceride concentration was monitored in calorie-restricted mice killed at the ages of 20, 30, or 40 weeks. **D:** Tissue contents of triglycerides (left), cholesterol (middle), and free fatty acids (right) were measured in epididymal fat pads collected from WT, Adipo-SIRT1, and Adipo-H363Y after 30 weeks of calorie restriction. **E:** Tissue triglyceride contents in livers and skeletal muscles collected from calorie-restricted WT, Adipo-SIRT1, and Adipo-H363Y were measured and compared ($n = 8$).

respectively, showed similar up- or downregulated patterns of change with those in old Adipo-SIRT1 when compared with young Adipo-SIRT1 (Supplementary Fig. 8, bottom panels).

Histone modifications control the stability and flexibility/rigidity of chromatin structure and its remodeling (24). Thus, histones were purified from adipose tissues of WT, Adipo-SIRT1, and Adipo-H363Y to analyze the modifications at the epigenetic levels. Western blotting showed that even at the young age (8 weeks old), the three types of mice contained different amounts of acetylated and/or biotinylated histones in their adipose tissues. Adipo-H363Y showed the highest level of histone biotinylation, whereas histone acetylation was significantly decreased in Adipo-SIRT1 (Fig. 5B). Coimmunoprecipitation was performed and the results further confirmed that histones, including H3 and H4, were acetylated and biotinylated in adipose tissues of the three groups of mice, with acetylated histones containing significantly higher amounts of biotinylation (Supplementary Fig. 9). Profile plots revealed that calorie restriction decreased the average gene expression levels in both old WT and old Adipo-H363Y (Fig. 5C), which was in line with the reduced histone acetylation levels in both types of

calorie-restricted mice (Fig. 5D). In addition, calorie restriction significantly decreased the biotinylation of histones in Adipo-H363Y preparations. By contrast, calorie restriction had no significant effects on histone acetylation and biotinylation in adipose tissues of Adipo-SIRT1, both of which were significantly lower than in those of Adipo-H363Y (Fig. 5D).

To confirm the altered epigenetic modifications in Adipo-H363Y, a number of genes were selected for analysis of the associated histones using ChIP-PCR. The expression of these genes, including *CUGBP*, *GADD*, *TRDN*, and *ADIPOQ*, was altered by aging and/or overexpression of hSIRT1(H363Y) (E-MTAB-2777 in ArrayExpress). Histone biotinylation was detected at the promoter regions of all four genes, and samples derived from Adipo-H363Y exhibited the highest levels of biotinylated histones (Supplementary Fig. 10, left panels). Consistent with gene expression changes induced by calorie restriction, the amount of biotinylated histones was significantly reduced in samples from calorie-restricted WT, Adipo-SIRT1, and Adipo-H363Y (Supplementary Fig. 10, right panels). The results further demonstrated that the amounts of biotinylated histones were significantly lower in fractions of nonacetylated than in those of acetylated histones (Supplementary Figs. 11 and 12).

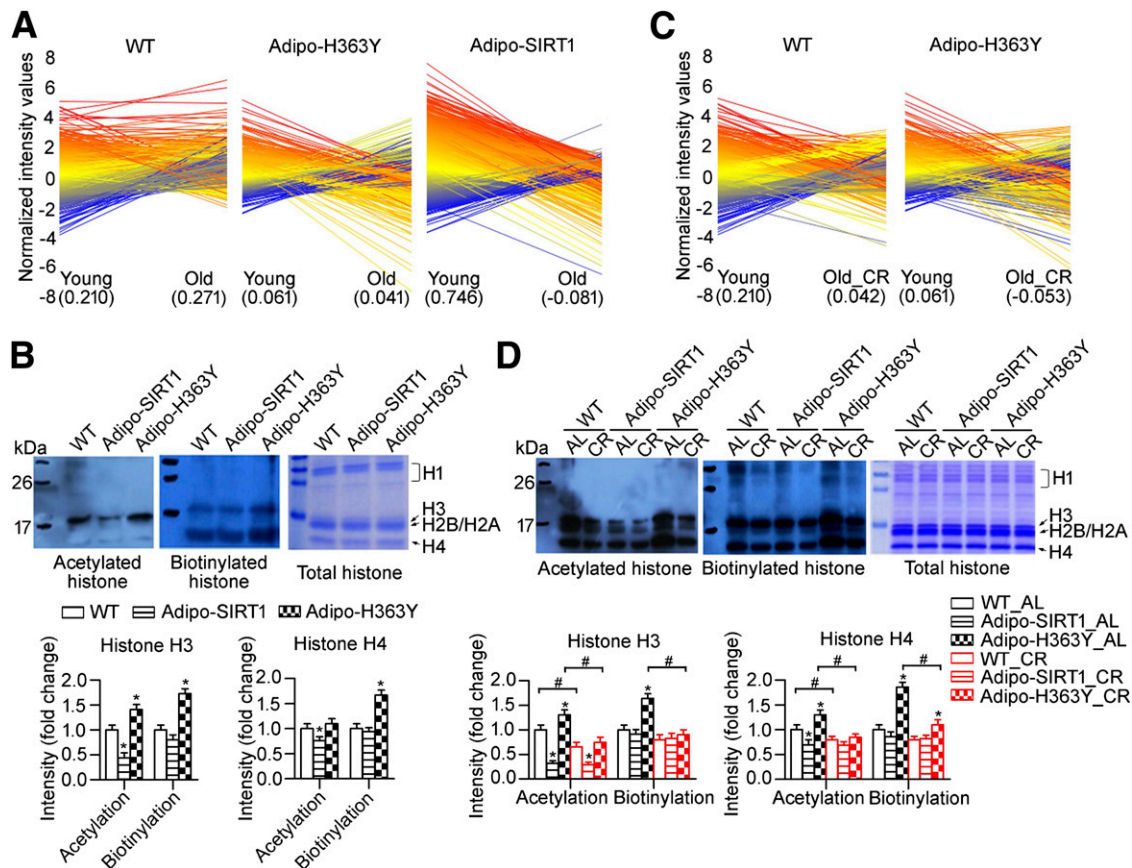


Figure 5—Calorie restriction prevents aging- and hSIRT1(H363Y)-induced gene changes by inhibiting histone biotinylation and promoting histone acetylation. **A:** Profile plot was performed by GeneSpring GX 12.6 to display the normalized intensity changes between young (8 weeks) and old (40 weeks) WT, Adipo-SIRT1, or Adipo-H363Y. Each line represents a single gene of the 3,915 gene list summary (Supplementary Table 1). The average intensities of all genes were calculated for both “young” and “old” samples and are listed at the bottom of each graph. **B:** Histone enrichment was performed using epididymal adipose tissues collected from 8-week-old WT, Adipo-SIRT1, and Adipo-H363Y. Western blotting was performed to analyze the global acetylated (top left, detected with antiacetylated lysine antibody) and biotinylated (top middle, probed with streptavidin-HRP) histone levels in isolated histone fractions (top right, stained with Coomassie Brilliant Blue). The band signals were quantified and presented as fold changes for H3 and H4, respectively (bottom left and right). **C:** Profile plot was performed as in Fig. 5A to display the normalized intensity changes between young (8 weeks) and calorie-restricted old (Old_CR, 40 weeks) WT or Adipo-H363Y. Each line represents a single gene of the 3,915 gene list (Supplementary Table 1). The average intensities of all genes were calculated and are listed at the bottom of each sample group. **D:** Epididymal fat pads were collected from mice (40 weeks old) that were either fed ad libitum (AL) or subjected to calorie restriction (CR). Global acetylated and biotinylated histone levels were determined as in panel B. * $P < 0.05$, compared with corresponding WT group; # $P < 0.05$, compared with corresponding AL group ($n = 3-6$).

Taken together, these results suggest that augmented histone biotinylation contributes to the rigid chromatin structure in adipose tissues of Adipo-H363Y, which prevents the adaptive responses of genomic activation and silencing, thus leading to an accelerated aging phenotype of these mice. The abnormal epigenetic modifications can be largely removed by calorie restriction.

Biotin Deficiency Prevents the Development of Metabolic Dysfunctions in WT and Adipo-H363Y

During aging, biotin is progressively accumulated in adipose tissues of mice and inhibits the deacetylase activity of SIRT1 (14). The biotin content in adipose tissues of Adipo-H363Y was augmented significantly (by approximately twofold) even at the age of 20 weeks when compared with those in WT (Fig. 6A, left panel). Calorie

restriction prevented the accumulation of biotin in adipose tissues of both WT and Adipo-H363Y (Fig. 6A, right panel). To further validate the involvement of biotin accumulation in adipose tissues as a cause of systemic metabolic deregulation, WT and Adipo-H363Y were given either a biotin-sufficient or a biotin-deficient diet from 10 to 20 weeks of age. This relatively short period of biotin deficiency did not induce obvious abnormalities but significantly reduced the biotin content and elevated SIRT1 activity in adipose tissues of WT and Adipo-H363Y (Fig. 6B). Compared with those receiving the biotin-sufficient diet, the amount of acetylated and biotinylated histones was decreased significantly in adipose tissues of mice fed the biotin-deficient diet (Fig. 6C). The latter diet also reduced the contents of the vitamin in livers

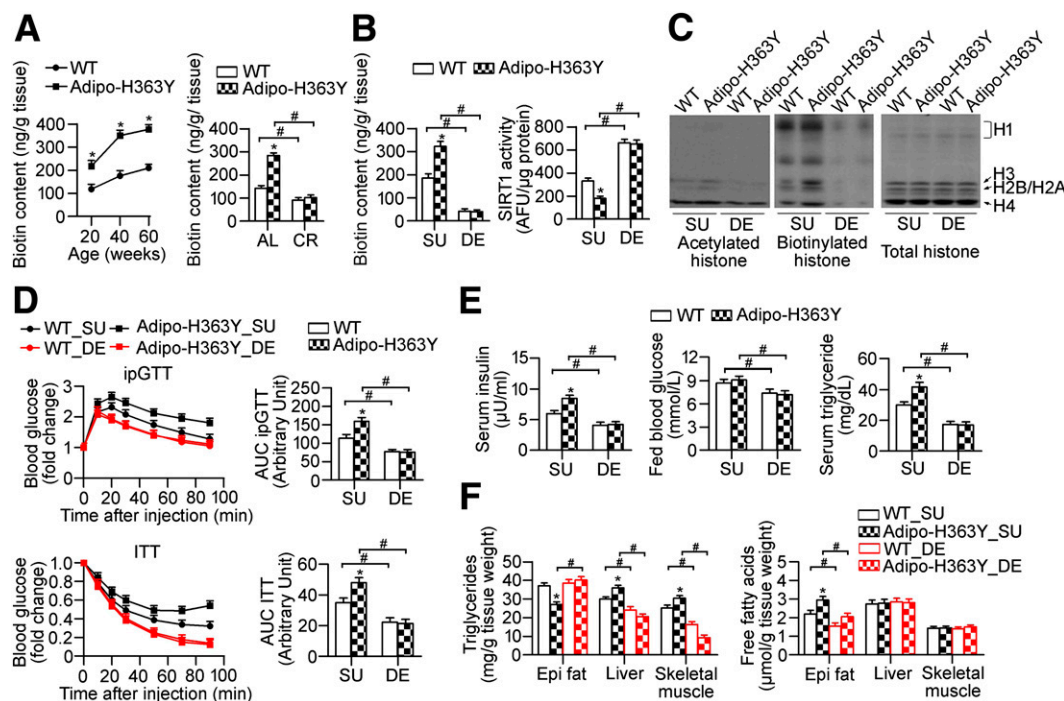


Figure 6—Biotin-deficient diet restores metabolic functions in WT and Adipo-H363Y. **A:** The tissue content of biotin was measured in epididymal fat pads collected from WT and Adipo-H363Y at different ages (left), and compared between mice (30 weeks old) that were fed ad libitum and under calorie restriction treatment (right). **B:** Biotin content (left) and SIRT1 activity (right) were measured in epididymal adipose tissues of WT and Adipo-H363Y subjected to treatments with biotin-sufficient (SU) or biotin-deficient (DE) diet. **C:** Acetylated or biotinylated histones were detected as in Fig. 5 using adipose tissues collected from WT and Adipo-H363Y fed with either SU or DE diets. **D:** ipGTT (top) and ITT (bottom) were performed in WT and Adipo-H363Y subjected to 10 weeks of SU or DE diets. The AUCs were calculated and compared (right panels). **E:** Serum insulin, nonfasting glucose, and circulating triglyceride levels were measured and compared in WT and Adipo-H363Y fed with SU or DE diets. **F:** Tissue triglycerides (left) and free fatty acids (right) were measured in WT and Adipo-H363Y fed with SU or DE diets. * $P < 0.05$, compared with corresponding WT control group; # $P < 0.05$, compared with the corresponding SU group ($n = 8$). AFU, arbitrary fluorescence unit.

(from 961 ± 113 to 703 ± 83 ng/g in WT and from $1,042 \pm 175$ to 685 ± 92 ng/g in Adipo-H363Y). By contrast, restriction of total calorie intake did not change the biotin contents in livers of either WT (710 ± 132 ng/g) or Adipo-H363Y (730 ± 111 ng/g), which were comparable to those of mice fed ad libitum (651 ± 98 and 680 ± 88 ng/g for WT and Adipo-H363Y, respectively).

Biotin-deficient mice exhibited significantly improved ipGTT and ITT responses compared with those receiving a biotin-sufficient diet (Fig. 6D). There was no significant difference between WT and Adipo-H363Y. The plasma insulin level was reduced in both WT and Adipo-H363Y fed with biotin-deficient diet (Fig. 6E, left panel). The nonfasting blood glucose was not different between WT and Adipo-H363Y receiving the biotin-sufficient diet, which contained higher amounts of sucrose (60%) and fat (12%) than the standard mouse chow (3.18 and 5.6%, respectively). Nevertheless, after ad libitum feeding with a biotin-deficient diet, the plasma glucose level was reduced in both WT and Adipo-H363Y (Fig. 6E, middle panel). Circulating triglycerides were also decreased by the biotin-deficient diet to similar levels in WT and Adipo-H363Y, when compared with their respective biotin-sufficient

groups (Fig. 6E, right panel). Likewise, the triglyceride content in skeletal muscle and liver was significantly reduced to comparable levels in biotin-deficient WT and Adipo-H363Y (Fig. 6F, left panel). Adipo-H363Y under biotin-deficient diet showed an enhanced capacity of triglyceride storage in their adipose tissues. In addition, the free fatty acid contents of adipose tissues were significantly reduced by the biotin-deficient diet in both WT and Adipo-H363Y (Fig. 6F, right panel). Both calorie restriction and the biotin-deficient diet increased SIRT1 protein expression in adipose tissues of WT but did not change that of Adipo-SIRT1 and Adipo-H363Y (Supplementary Fig. 13A). The circulating adiponectin levels were elevated by both calorie restriction and the biotin-deficient diet, whereas the circulating levels of the proinflammatory adipokine lipocalin-2 were reduced by these treatments (Supplementary Fig. 13B and C).

Taken in conjunction, the present results support the concept that biotin accumulation in adipose tissue is causally involved in the development of aging-associated metabolic abnormalities and, thus, that limiting the intake of biotin represents an effective way to enhance adipose SIRT1 function and prevent metabolic aging.

Upregulated Acetyl-CoA Carboxylase 2 Contributes to the Dominant-Negative Effects of hSIRT1(H363Y) on Inhibiting Endogenous SIRT1

SIRT1 regulates the protein stability and acetylation status of acetyl-CoA carboxylase (ACC), a biotin reservoir (14,25). The protein expression of ACC was upregulated in adipose tissues of Adipo-H363Y (Fig. 7A). Further analysis revealed that the total protein level of isoform ACC2, but not ACC1, and that of acetylated ACC2 were augmented significantly in adipose tissues of Adipo-H363Y (Supplementary Fig. 14A). Both SIRT1 and ACC2 were present in mitochondria isolated from the three groups of mice (Supplementary Fig. 14B). Both calorie restriction and biotin-deficient diet decreased the total amount of ACC2 in adipose tissues of Adipo-H363Y (Fig. 7B). The amount of acetylated ACC2 was also reduced by the treatments (Fig. 7C). To confirm that ACC2 is involved in regulating the total amount of biotin, specific chemically

modified ACC2 siRNAs were used to treat WT and Adipo-H363Y in vivo. After treatment, epididymal adipose tissues were collected for analysis. Reducing total ACC2 protein levels significantly decreased the amount of biotin in adipose tissues of both types of mice but increased their SIRT1 activities (Fig. 7D). Moreover, ACC2 siRNA treatment significantly inhibited the biotinylation and acetylation of histones in adipose tissues of Adipo-H363Y (Fig. 7E). In addition, recombinant adenovirus-mediated overexpression of hSIRT1(H363Y) in cultured 3T3-L1 adipocytes significantly increased the protein levels of ACC2, the intracellular accumulation of biotin, as well as the amount of biotinylated histones (Fig. 7F).

Histones are the most conserved protein substrates of SIRT1 (26). To define the interrelationships between histone acetylation and biotinylation, a series of histone H3 peptides containing 21 amino acid residues with acetylated K14 and/or biotinylated K18 was synthesized

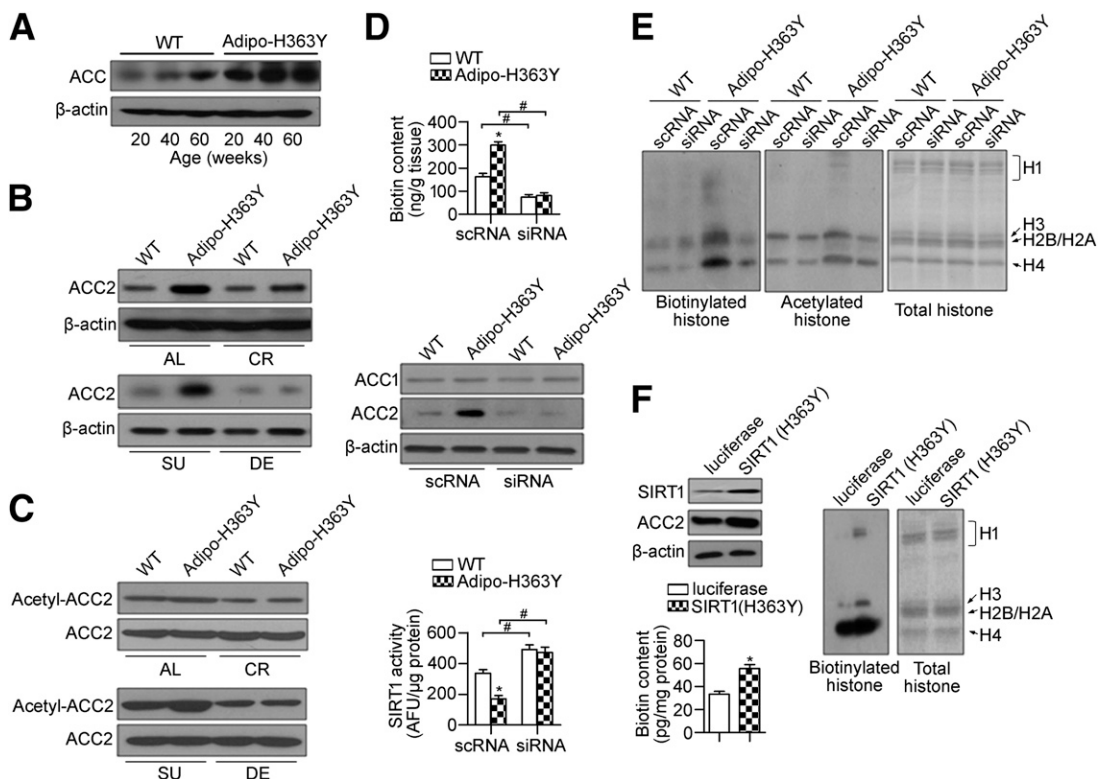


Figure 7—ACC2 regulates total biotin content in adipose tissues. **A**: Western blotting analysis of ACC protein expression in epididymal fat pads collected from WT and Adipo-H363Y at different ages. **B**: Expression of ACC2 was compared in epididymal fat pads of WT and Adipo-H363Y fed ad libitum (AL) or under calorie restriction (CR) (top), or subjected to biotin-sufficient (SU) or biotin-deficient (DE) diet treatments (bottom). **C**: Immunoprecipitation was performed using antibodies against ACC2 and the acetylated ACC2 was measured in the immunoprecipitates by Western blotting. **D**: Biotin content (top), ACC expressions (middle), and SIRT1 activity (bottom) were measured in epididymal fat lysates of WT and Adipo-H363Y treated in vivo with specific ACC2 siRNA or scrambled siRNA (scRNA). **E**: Biotinylated and acetylated level of histones were compared in epididymal fat pads of WT and Adipo-H363Y after RNAi treatment as in panel **D**. **F**: Murine 3T3-L1 preadipocytes induced to differentiate as previously described (50), followed by infection with recombinant adenoviruses encoding luciferase or the human SIRT1 mutant hSIRT1(H363Y) at a multiplicity of infection of 100 (51). The cells were harvested 48 h after infection. Protein expression of SIRT1 and ACC2 (top left), biotin content (bottom left), and biotinylated histones (right) were measured as above. AFU, arbitrary fluorescence unit. * $P < 0.05$, compared with corresponding control groups; # $P < 0.05$, compared with the corresponding scRNA groups ($n = 3-4$).

(Supplementary Fig. 15A). In vitro deacetylation assays were performed to compare SIRT1-mediated deacetylation of acetyl-H3 with that of biotinyl-acetyl-H3 (Supplementary Fig. 15B). The ratios of nicotinamide (NAM) to NAD and deacetyl-H3 to acetyl-H3, which were calculated based on the sizes of the peaks, were both significantly reduced (by ~80%) in reactions containing the peptide with biotinylated K18 (Supplementary Fig. 15B), indicating that biotinylated histones are less susceptible to SIRT1-mediated deacetylation. When biotin was present in the reaction buffer, SIRT1 did not cause deacetylation of acetyl-H3 peptide (Supplementary Fig. 15C). In fact, the addition of biotin facilitated the formation of biotinyl-acetyl-H3 peptide clusters from acetyl-H3 peptide (Supplementary Fig. 15C).

These results demonstrate that upregulated ACC2 in adipose tissues of Adipo-H363Y plays a major role in causing accumulation of biotin, which either directly inhibits the endogenous SIRT1 activity (14) or promotes histone biotinylation, in turn preventing SIRT1-mediated deacetylation.

DISCUSSION

Adipose tissue stores the surplus of energy as triglycerides and regulates whole-body energy metabolism by secreting adipokines that elicit endocrine/paracrine functions. During aging, the distribution and composition of body fat change significantly (27). A decline of fat storage in adipose depots and an elevation of fat accumulation in ectopic organs (e.g., liver and skeletal muscle) contribute to the deterioration of systemic metabolic functions, including insulin resistance, hyperlipidemia, and hyperglycemia (28). Overflow of lipids into organs other than the fat depots is also a significant contributing factor to the accelerated aging process in obese populations (29). Calorie restriction is the most robust nongenetic approach to extend life span and improve health in mammals (30). It counteracts obesity and related metabolic complications by promoting weight loss and normalizing the function of adipose tissues (31). In particular, calorie restriction increases the production of adiponectin, an insulin-sensitizing adipokine (32), and represses inflammation in adipose tissues (33). Yet, the molecular mechanisms underlying the beneficial effects of calorie restriction are still poorly understood. It has been questioned whether the actual decrease in calorie intake or the restriction of varying nutrients accounts for life span modulation by calorie restriction (34).

The current study demonstrates that restricting certain dietary components, in particular biotin, impacts positively on energy metabolism and prevents metabolic aging, by enhancing SIRT1 activities in adipose tissues. Biotin and its metabolite, biotinyl-5'-AMP, are potent and competitive inhibitors of SIRT1 (14). Biotinyl-5'-AMP occupies the NAD binding site and prevents the breakdown of NAD by SIRT1. Since NAD also acts as a cofactor permitting SIRT1 to interact with protein substrates,

inhibition of NAD binding by biotinyl-5'-AMP prevents the interactions between SIRT1 and acetylated protein substrates (14). Biotin occupies the binding pocket of NAM, which may prevent the conformational change from nonproductive to productive SIRT1 (35,36). Calorie restriction reduces total biotin levels in adipose tissues; as a result, the direct inhibitory effects of this vitamin on SIRT1 activity in such tissues of calorie-restricted WT and Adipo-H363Y are alleviated.

The present results further suggest that biotinylation of protein substrates represents an indirect route by which biotin interferes with the enzymatic functions of SIRT1. Biotinylated histone peptides are resistant to SIRT1-mediated deacetylation. Although being relatively rare (37), biotinylated histones have been detected in human cells and play a functional role in gene silencing, responses to DNA damage, and cell proliferation (38). Spontaneous histone biotinylation occurs in the presence of biotinyl-5'-AMP and in the absence of biotin protein ligases (39). Thus, an increased intracellular biotin content and/or turnover can elevate the amount of biotinylated histones. So far, 11 biotinylation sites in histones have been identified, including K9, 13, 125, 127, and 129 in histone H2A; K4, 9, 18, and 23 in histone H3; and K8 and 12 in histone H4 (40). Biotinylated histones contribute to epigenetic modulations involved in the regulation of chromatin structure/stability and genome activation/inactivation. This conclusion is supported by the present observation that different levels of histone biotinylation determine the distinctive patterns of aging-induced chromatin remodeling. Biotin-containing nucleosomes maintain a more condensed average structure (41). In Adipo-H363Y, increased biotinylation prevents endogenous SIRT1-mediated deacetylation of histones and renders the genome more rigid even at a relatively young age. The resulting structural changes alter the chromatin activities of Adipo-H363Y, causing an imbalanced production of pro- and anti-inflammatory adipokines, abnormal expression of genes involved in lipid metabolism, adipogenesis and extracellular matrix deposition, and aberrant genetic adaptations to external conditions and aging. However, calorie restriction can restore the nucleosomal remodeling process and reset the basal state of the genome structures in adipose tissues of Adipo-H363Y. The current study further demonstrates that the beneficial effects of calorie restriction can be mimicked by restriction intake of biotin, which directly (14) and indirectly (by modifying its protein substrates) enhances the endogenous activity of SIRT1.

The initial breakthrough of identification of SIR2 as an enzyme came along with the identification of the *Salmonella typhimurium* CobB protein, a SIR2 homolog (42). CobB compensates for the lack of CobT mutants during vitamin B12 biosynthesis and possesses nicotinate mononucleotide (NaMN)-dependent phosphoribosyltransferase activity. Thus, CobB catalyzes the release of nicotinic acid from NaMN, whereas SIRT1 removes

NAM from NAD. Biotin and NAM were originally discovered as the same class of heat-stable vitamins (43). Unlike NAM, nutritional deficiencies of biotin are rare. Biotin functions in mammals as a CO₂ carrier for reactions in which a carboxyl group is transferred to one of four biotin-dependent carboxylases. Consequently, biotin participates as an important cofactor in gluconeogenesis, fatty acid synthesis, and branched-chain amino acid catabolism (44). During aging, the deacetylase activity of SIRT1 is decreasing progressively in adipose tissues, and this is accompanied by excessive biotin accumulation (14). The evidence from the current study and a previous report suggests that biotin supply in diet dominantly inhibits SIRT1 activity and abolishes the beneficial functions of this antiaging protein (14). However, a self-defending mechanism for preventing excess accumulation of biotin is controlled by SIRT1 via ACC2, a major intracellular reservoir and a mitochondrial store of biotin (14,45). The present results suggest that by reducing the total protein amount of ACC2, SIRT1 can regulate the intracellular biotin contents in adipocytes. Under conditions of low biotin intake, enhanced SIRT1 activity downregulates ACC2, leading to a further decrease of intracellular biotin content and the elimination of biotinylated histones, in turn facilitating the dynamic chromatin remodeling and genome activation/inactivation.

The highly conserved H363 residue of SIRT1 forms the binding site for NAD. In yeast, the hSIRT1(H363Y) equivalent mutant SIR2(H364Y) possesses an impaired NAD-dependent histone deacetylase activity (7,26). The strong dominant-negative effects of SIR2(H364Y) have been suggested to result from the incorporation of an inactive SIR2 into silencing complexes. In mammalian cells, whereas the histone deacetylation activity of hSIRT1(H363Y) is impaired, the silencing effects of this mutant are not completely lost (46,47). The hSIRT1(H363Y) mutant exhibits defective substrate binding and catalytic activity that are not locus or species specific (35). The current study reveals that in adipose tissues of Adipo-H363Y, increased biotin contents and augmented biotinylation of histones play a dominant-negative role in preventing endogenous SIRT1-mediated deacetylation and chromatin remodeling. In adipose tissues of Adipo-SIRT1, the interactions between SIRT1 and ACC2 are significantly enhanced and more sensitive to nutritional changes. By contrast, mice with overexpression of hSIRT1(H363Y) in adipose tissues show significantly decreased interactions between ACC2 and SIRT1 (data not shown), leading to a persistent elevation of the protein levels of ACC2, both under basal conditions and during dietary interventions. The present results demonstrate that downregulation of ACC2 (the mitochondrial form of ACC [48]) reduces the biotin content in adipose tissues and leads to a significantly decreased level of histone biotinylation. Previous radioactive tracer studies suggest that a significant portion of biotin is localized as bound forms in both nuclei and mitochondria (49). Whereas ACC2 and SIRT1 are both localized in

mitochondria, the amount of SIRT1(H363Y) in this organelle is significantly reduced, which may be attributed to the augmented ACC2 protein levels in adipose tissues of these mice.

In summary, histone biotinylation was significantly enhanced in adipose tissues of Adipo-H363Y, causing deranged epigenetic modifications and chromatin remodeling, which contributed to the accelerated aging phenotype in these mice. Calorie restriction reduces biotinylated histone levels in adipose tissues of Adipo-H363Y, allowing nucleosome deacetylation to occur in these mice at similar levels as in WT. However, unlike biotin-deficient diet, calorie restriction could not further improve most of the metabolic parameters beyond the levels of those in Adipo-SIRT1, which correlates with its milder effects on biotin reduction in mouse adipose tissues. By contrast, the biotin-deficient diet more aggressively decreases biotin contents in adipose tissues of WT and Adipo-H363Y beyond those in Adipo-SIRT1, supporting the interpretation that short-term biotin restriction in the diet is more effective in improving metabolic function than a general restriction of total calorie intake. Thus, although biotinylation directly inhibits SIRT1-mediated deacetylation of histones, calorie restriction or a diet deficient in biotin prevents histone biotinylation independent of SIRT1, which subsequently facilitates gene silencing and prevents aging (Fig. 8). Based on this information, one could speculate that in mammals, caloric restriction may enhance SIRT1 activity by selective depletion of biotin storage in adipose tissue, in turn preventing aging-associated metabolic disorders and promoting life span extension.

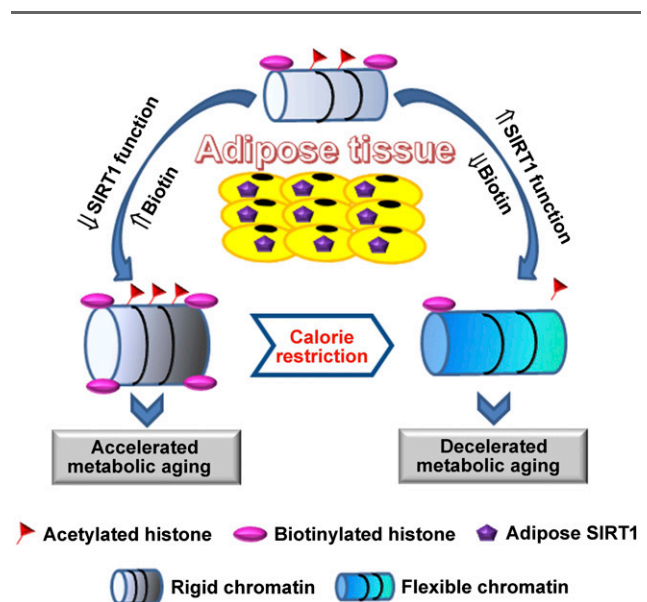


Figure 8—Schematic summary. Calorie restriction prevents SIRT1 dysfunction-induced abnormal chromosome remodeling and epigenetic modification in adipose tissues.

Funding. This work was supported in part by grants from Seeding Funds for Basic Research of The University of Hong Kong, Research Grant Council grants (HKU779712M and HKU780613M) of Hong Kong, the Special Equipment Grant Scheme (SEGHKU02) from University Grants Committee, HKSAR, and the National Basic Research Program of China (973 Program 2015CB553603).

Duality of Interest. No potential conflicts of interest relevant to this article were reported.

Author Contributions. C.X. performed the experiments, analyzed the data, presented the results, and prepared the manuscript. Y.C. and P.F. performed the experiments, analyzed the data, and presented the results. B.B. and J.C. performed the experiments. H.-B.D. analyzed the data and presented the results. C.-M.C. obtained funding support and revised the manuscript. A.X. obtained funding support, designed the experiments, supervised the project, and revised the manuscript. P.M.V. obtained funding support, designed the experiments, supervised the project, and prepared and revised the manuscript. Y.W. obtained funding support, designed the experiments, supervised the project, analyzed data and presented the results, and prepared and revised the manuscript. Y.W. is the guarantor of this work and, as such, had full access to all the data in the study and takes responsibility for the integrity of the data and the accuracy of the data analysis.

References

- Jamali R, Bachrach-Lindström M, Mohseni S. Continuous glucose monitoring system signals the occurrence of marked postprandial hyperglycemia in the elderly. *Diabetes Technol Ther* 2005;7:509–515
- Kalyani RR, Egan JM. Diabetes and altered glucose metabolism with aging. *Endocrinol Metab Clin North Am* 2013;42:333–347
- Russell SJ, Kahn CR. Endocrine regulation of ageing. *Nat Rev Mol Cell Biol* 2007;8:681–691
- Tchkonina T, Thomou T, Zhu Y, et al. Mechanisms and metabolic implications of regional differences among fat depots. *Cell Metab* 2013;17:644–656
- Wang Y, Xu C, Liang Y, Vanhoutte PM. SIRT1 in metabolic syndrome: where to target matters. *Pharmacol Ther* 2012;136:305–318
- Wang Y. Molecular links between caloric restriction and Sir2/SIRT1 activation. *Diabetes Metab J* 2014;38:321–329
- Tanny JC, Dowd GJ, Huang J, Hilz H, Moazed D. An enzymatic activity in the yeast Sir2 protein that is essential for gene silencing. *Cell* 1999;99:735–745
- Frye RA. Characterization of five human cDNAs with homology to the yeast SIR2 gene: Sir2-like proteins (sirtuins) metabolize NAD and may have protein ADP-ribosyltransferase activity. *Biochem Biophys Res Commun* 1999;260:273–279
- Chalkiadaki A, Guarente L. Sirtuins mediate mammalian metabolic responses to nutrient availability. *Nat Rev Endocrinol* 2012;8:287–296
- Corbi G, Conti V, Scapagnini G, Filippelli A, Ferrara N. Role of sirtuins, calorie restriction and physical activity in aging. *Front Biosci (Elite Ed)* 2012;4:768–778
- Cohen HY, Miller C, Bitterman KJ, et al. Calorie restriction promotes mammalian cell survival by inducing the SIRT1 deacetylase. *Science* 2004;305:390–392
- Picard F, Kurtev M, Chung N, et al. Sirt1 promotes fat mobilization in white adipocytes by repressing PPAR-gamma. *Nature* 2004;429:771–776
- Chen D, Bruno J, Easlson E, et al. Tissue-specific regulation of SIRT1 by calorie restriction. *Genes Dev* 2008;22:1753–1757
- Xu C, Bai B, Fan P, et al. Selective overexpression of human SIRT1 in adipose tissue enhances energy homeostasis and prevents the deterioration of insulin sensitivity with ageing in mice. *Am J Transl Res* 2013;5:412–426
- Bordone L, Cohen D, Robinson A, et al. SIRT1 transgenic mice show phenotypes resembling calorie restriction. *Aging Cell* 2007;6:759–767
- Banks AS, Kon N, Knight C, et al. SirT1 gain of function increases energy efficiency and prevents diabetes in mice. *Cell Metab* 2008;8:333–341
- Kraus D, Yang Q, Kong D, et al. Nicotinamide N-methyltransferase knockdown protects against diet-induced obesity. *Nature* 2014;508:258–262
- Law IK, Xu A, Lam KS, et al. Lipocalin-2 deficiency attenuates insulin resistance associated with aging and obesity. *Diabetes* 2010;59:872–882
- Wang Y, Lam KS, Chan L, et al. Post-translational modifications of the four conserved lysine residues within the collagenous domain of adiponectin are required for the formation of its high molecular weight oligomeric complex. *J Biol Chem* 2006;281:16391–16400
- Wang Y, Lam KS, Kraegen EW, et al. Lipocalin-2 is an inflammatory marker closely associated with obesity, insulin resistance, and hyperglycemia in humans. *Clin Chem* 2007;53:34–41
- Chow KH, Sun RW, Lam JB, et al. A gold(III) porphyrin complex with anti-tumor properties targets the Wnt/beta-catenin pathway. *Cancer Res* 2010;70:329–337
- Peng GH, Chen S. Double chromatin immunoprecipitation: analysis of target co-occupancy of retinal transcription factors. *Methods Mol Biol* 2013;935:311–328
- Hayakawa K, Oizumi J. Determination of free biotin in plasma by liquid chromatography with fluorimetric detection. *J Chromatogr A* 1987;413:247–250
- Fang WQ, Ip JP, Li R, et al. Cdk5-mediated phosphorylation of Axin directs axon formation during cerebral cortex development. *J Neurosci* 2011;31:13613–13624
- Law IK, Liu L, Xu A, et al. Identification and characterization of proteins interacting with SIRT1 and SIRT3: implications in the anti-aging and metabolic effects of sirtuins. *Proteomics* 2009;9:2444–2456
- Imai S, Armstrong CM, Kaeberlein M, Guarente L. Transcriptional silencing and longevity protein Sir2 is an NAD-dependent histone deacetylase. *Nature* 2000;403:795–800
- Tchkonina T, Morbeck DE, Von Zglinicki T, et al. Fat tissue, aging, and cellular senescence. *Aging Cell* 2010;9:667–684
- Ahima RS. Connecting obesity, aging and diabetes. *Nat Med* 2009;15:996–997
- Tzanetakou IP, Katsilambros NL, Benetos A, Mikhailidis DP, Perrea DN. “Is obesity linked to aging?”: adipose tissue and the role of telomeres. *Ageing Res Rev* 2012;11:220–229
- Mattison JA, Roth GS, Beasley TM, et al. Impact of caloric restriction on health and survival in rhesus monkeys from the NIA study. *Nature* 2012;489:318–321
- Liao CY, Rikke BA, Johnson TE, Gelfond JA, Diaz V, Nelson JF. Fat maintenance is a predictor of the murine lifespan response to dietary restriction. *Aging Cell* 2011;10:629–639
- Wang Y, Lam KS, Yau MH, Xu A. Post-translational modifications of adiponectin: mechanisms and functional implications. *Biochem J* 2008;409:623–633
- Ding Q, Ash C, Mracek T, Merry B, Bing C. Caloric restriction increases adiponectin expression by adipose tissue and prevents the inhibitory effect of insulin on circulating adiponectin in rats. *J Nutr Biochem* 2012;23:867–874
- Szafranski K, Mekhail K. The fine line between lifespan extension and shortening in response to caloric restriction. *Nucleus* 2014;5:56–65
- Min J, Landry J, Sternglanz R, Xu RM. Crystal structure of a SIR2 homolog-NAD complex. *Cell* 2001;105:269–279
- Zhao K, Harshaw R, Chai X, Marmorstein R. Structural basis for nicotinamide cleavage and ADP-ribose transfer by NAD(+)-dependent Sir2 histone/protein deacetylases. *Proc Natl Acad Sci U S A* 2004;101:8563–8568
- Kuroishi T, Rios-Avila L, Pestinger V, Wijeratne SS, Zemljeni J. Biotinylation is a natural, albeit rare, modification of human histones. *Mol Genet Metab* 2011;104:537–545
- Filenko NA, Kolar C, West JT, et al. The role of histone H4 biotinylation in the structure of nucleosomes. *PLoS ONE* 2011;6:e16299
- Healy S, Heightman TD, Hohmann L, Schriemer D, Gravel RA. Nonenzymatic biotinylation of histone H2A. *Protein Sci* 2009;18:314–328
- Zemljeni J, Teixeira DC, Kuroishi T, Cordonier EL, Baier S. Biotin requirements for DNA damage prevention. *Mutat Res* 2012;733:58–60
- Singh MP, Wijeratne SS, Zemljeni J. Biotinylation of lysine 16 in histone H4 contributes toward nucleosome condensation. *Arch Biochem Biophys* 2013;529:105–111
- Tsang AW, Escalante-Semerena JC. CobB, a new member of the SIR2 family of eucaryotic regulatory proteins, is required to compensate for the lack of

nicotinate mononucleotide:5,6-dimethylbenzimidazole phosphoribosyltransferase activity in cobT mutants during cobalamin biosynthesis in *Salmonella typhimurium* LT2. *J Biol Chem* 1998;273:31788–31794

43. Lanska DJ. The discovery of niacin, biotin, and pantothenic acid. *Ann Nutr Metab* 2012;61:246–253

44. Depeint F, Bruce WR, Shangari N, Mehta R, O'Brien PJ. Mitochondrial function and toxicity: role of the B vitamin family on mitochondrial energy metabolism. *Chem Biol Interact* 2006;163:94–112

45. Shriver BJ, Roman-Shriver C, Allred JB. Depletion and repletion of biotinyl enzymes in liver of biotin-deficient rats: evidence of a biotin storage system. *J Nutr* 1993;123:1140–1149

46. Senawong T, Peterson VJ, Leid M. BCL11A-dependent recruitment of SIRT1 to a promoter template in mammalian cells results in histone deacetylation and transcriptional repression. *Arch Biochem Biophys* 2005;434:316–325

47. Langley E, Pearson M, Faretta M, et al. Human SIR2 deacetylates p53 and antagonizes PML/p53-induced cellular senescence. *EMBO J* 2002;21:2383–2396

48. Abu-Elheiga L, Matzuk MM, Abo-Hashema KA, Wakil SJ. Continuous fatty acid oxidation and reduced fat storage in mice lacking acetyl-CoA carboxylase 2. *Science* 2001;291:2613–2616

49. Dakshinamurti K. Biotin—a regulator of gene expression. *J Nutr Biochem* 2005;16:419–423

50. Wang Y, Xu A, Knight C, Xu LY, Cooper GJ. Hydroxylation and glycosylation of the four conserved lysine residues in the collagenous domain of adiponectin. Potential role in the modulation of its insulin-sensitizing activity. *J Biol Chem* 2002;277:19521–19529

51. Zu Y, Liu L, Lee MY, et al. SIRT1 promotes proliferation and prevents senescence through targeting LKB1 in primary porcine aortic endothelial cells. *Circ Res* 2010;106:1384–1393